1896 *Russian Chemical Bulletin, Vol. 47, No. 10, October, 1998*

Effect of acridine hydrochloride on the temperature dependence of dissolution of Sn70In alloy

V. V. Ekilik, A. G. Berezhnaya, and M. G. Komakhidze*

Rostov State University,
7 ul. Zorge, 344090 Rostov-on-Don, Russian Federation.
Fax: +7 (863 2) 64 5255. E-mail: elchim@chimfak.rnd.runnet.ru

The effects of temperature, potential, and addition of acridine hydrochloride on the anodic dissolution of SnIn alloy containing 70% In in a chloride-containing solution were studied by chronoamperometry. The processes of In dissolution limited by solid and liquid state diffusions and also those associated with a phase rearrangement and enhancement of the alloy surface were considered.

Key words: tin—indium alloy, acridine hydrochloride, selective dissolution.

Unlike binary alloys with a low or medium content of the more electronegative component $[A]_0$, alloys with high $[A]_0$ are much less studied,[1—3] and data on the influence of the temperature on the rate of dissolution of these alloys, including those in solutions containing surfactants added, are missing. In this work, we studied the influence of the temperature on the selective dissolution of an indium—tin alloy in the presence of acridine hydrochloride and the enhancement of the alloy surface caused by the phase rearrangement.

Experimental procedure

The anodic dissolution of Sn70In alloy with a content of indium $[\mathrm{In}]_0$ of 70% (w/w) was studied by the potentiostatic method with a stationary electrode in argon-saturated solutions containing 1 *M* LiCl + 0.01 *M* HCl at potentials $E = -0.58$ and -0.52 V (*vs* saturated silver chloride electrode) in the 25—65 °C temperature range. The velocity of hydrogen evolution found by extrapolation of the cathodic curve was smaller than the anodic current density (I_a) by more than three orders of magnitude. The rate of tin dissolution determined by polarography was smaller than I_a by 2.5 orders of magnitude. Therefore, it was assumed that the partial rate of indium dissolution $i_{\mathrm{In}} \approx I_a$. The experimental procedure and pretreatment of the electrodes were described in more detail in a previous publication.[4] Acridine hydrochloride (AHC) in a concentration of 5 mmol L^{-1} was used as the additive.

Results and Discussion

SnIn alloys are reversibly dissolved in chloride media;[5] this involves successive replacement of retarded diffusion steps of the process by one another and can be accompanied by phase rearrangements.[2,3] Based on these data, the anodic current—time transients obtained for the dissolution of In from the Sn70In alloy can be divided into several sections (*1—7*), in accordance with the scheme shown in Fig. 1.

The transition time $\tau_{t,1}$ ($s^{1/2}$) (see Fig. 1) corresponds to the replacement of retarded unsteady-state liquid diffusion (section *1—2*) by retarded steady-state liquid diffusion (section *2—3*) ($\tau_{t,2}$). Section *3—4* is described by Eq. (1) [2,6] and corresponds to the region of mixed kinetics in which the rates of steady-state liquid diffusion and unsteady-state solid diffusion are commensurable.

$$i_{\mathrm{In}} = P - Q\tau^{1/2}, \qquad (1)$$

$$P = n_A F D_{\mathrm{In}^{3+}} [\mathrm{In}]_S \delta^{-1} \exp(2,3\Delta E_0/b_a), \qquad (2)$$

$$Q = 2P^2/(n_A F[\mathrm{In}]_S \sqrt{\pi D_{\mathrm{In}}}\ ), \qquad (3)$$

where P/A m^2 and Q/A (m^2 s$^{1/2}$)$^{-1}$ are coefficients of the linear Eq. (*1*); $D_{\mathrm{In}^{3+}}$ and D_{In} are the liquid and solid-state diffusion coefficients, respectively, F/C (g-equiv.)$^{-1}$ is the Faraday constant; δ is the thickness of the liquid diffusion layer, $[\mathrm{In}]_S$ is the surface concentration of In in the solid phase, $\Delta E_0 = E - E_p^0$, E_p^0 is the standard reversible In^{3+}/In potential; and b_a/B is the Tafel coefficient.

The surface enhancement caused by the phase rearrangement occurs after τ_{se}. The competing influence of two factors, namely, the increase in the thickness of the solid-state diffusion layer with time due to the selective dissolution of the alloy and the surface enhancement leading to the appearance of areas with increased $[\mathrm{In}]_S$ on the bottom of cracks, on the i_{In} value results in a multiextremum dependence of i_{In} on τ in section *4—7*.[6]

It can be seen from Table 1 that the anodic behavior of the alloy depends on the potential E. The presence of extrema on the current—time transients is more typical at $E = -0.52$ V; in other words, in this case, the phase

Translated from *Izvestiya Akademii Nauk. Seriya Khimicheskaya,* No. 10, pp. 1950—1954, October, 1998.

1066-5285/98/4710-1896 $20.00

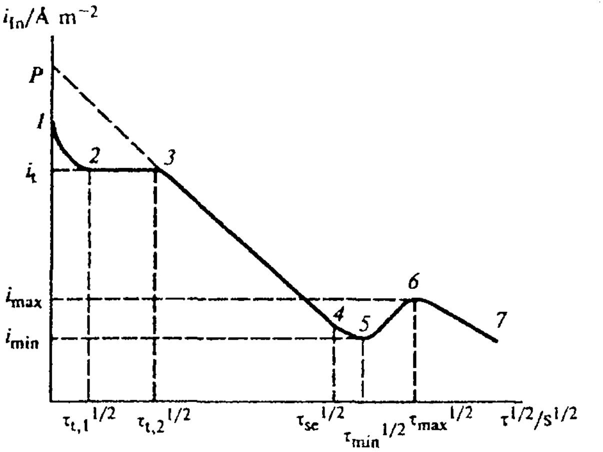

Fig. 1. Scheme for the anodic current—time transient for the dissolution of indium from the alloy: (*1—7*) stages of the process and phase rearrangements; i_{In} is the rate of indium dissolution, and $\tau^{1/2}$ is the phase rearrangement time.

rearrangement and the surface enhancement occur more intensely, whereas sections *1—2* and *2—3* are not realized. In addition, when E increases, the efficiency of AHC diminishes (see below).

Since at higher temperatures (T) i_{In} increases, this should increase the concentration of irreversible vacancies and the defectiveness of the surface layer; in addition, this should facilitate the phase rearrangement and the surface enhancement. In fact, as the temperature is raised, the current characteristics i_{se}, i_{max}, i_{min}, and i_{max}/i_{min} increase, whereas τ_{se} and q_{se} decrease. The unit critical electric charge q_{se} is supplied to the electrode over time τ_{se}, which can be interpreted as the induction period of surface enhancement. Since upon an increase in T, the relaxation after the phase rearrangement occurs faster and is characterized by a smaller q_{se}, of the two processes, *viz.*, generation and drain of vacancies resulting in the formation of the irreversible surface layer, the former is accelerated to a larger extent with an increase in T.

Since i_{max}/i_{min} is not larger than 1.4 at $E = -0.52$ V, the surface enhancement is relatively insignificant and becomes somewhat more pronounced as T increases. During the period $\Delta\tau_1$, the decrease in the rate of solid-state diffusion predominates over the increase in i_{In} due to the surface enhancement. In the $\Delta\tau_2$ range, the second factor starts to predominate. At τ_{min} and τ_{max}, these factors are equally significant. The increase in $\Delta\tau_1$ and the decrease in $\Delta\tau_2$ following an increase in T implies that the temperature has a greater effect on the solid-state diffusion than on the phase rearrangement or the surface enhancement.

At $E = -0.58$ V, the temperature dependences of τ_{se}, i_{se}, and q_{se} are similar. As should be expected, at this potential, the i_{se} values are smaller, whereas the τ_{se} values are higher than the corresponding values at $E = -0.52$ V. However, according to the data reported previously,[3,6] the q_{se} value is virtually invariant with respect to E over the T range considered.

The dependence of i_{In} on T is linearized in the Arrhenius coordinates, $\log i_{In}$—$1/T$. To calculate the activation energy (W) more correctly, it is necessary that a given τ be matched by equal sections in the current—time transients, *i.e.*, that the retarded stage of the process be retained. Therefore, several W values for sections that overlapped in time were calculated (Table 2).

The W values for section *3—4* of the mixed kinetics lie mostly in the 20±4 kJ mol^{-1} range; they scarcely depend on the E value and somewhat decrease with τ. The transition to the dissolution of In under the conditions of phase rearrangement and surface enhancement is accompanied by a substantial decrease in the W values, as indicated by the comparison of their values found for identical τ but different T ranges. At $E = -0.58$ V, surface enhancement is less significant and the W values become somewhat larger than those at $E = -0.52$ V.

To estimate the temperature dependence of the solid-state diffusion rate, we used the Arrhenius equation (4) and the D_{In} values (see Table 1), which do not depend on the time τ when $\tau < \tau_{se}$ and had been calculated using Eq. (6),[6] which follows from Eqs. (2) and (3).

$$D_{In} = D_{In}{}^{0}\exp[-W_D/(RT)], \quad (4)$$

$$D_{In}{}^{0} = \nu\exp(\Delta S/R), \quad (5)$$

$$D_{In} = 4P^4(9Q^2\pi F^2[\mathrm{In}]_0{}^2), \quad (6)$$

where ΔS is the activation entropy and ν is the frequency of thermal collisions of particles.

It follows from Table 3 that the W_D value in a solution containing no AHC virtually does not depend on the E value, while the entropy factor increases with an increase in E. According to the mechanism of diffusion through irreversible vacancies,[1—3] the effect of AHC on the constituents of D_{In} is determined by the E value and is formed in an initial time interval.

In the general case, the addition of inhibitors can retard the reversible dissolution of alloy components as a result of complexation, by forming a polymolecular film on the surface, or by decreasing the liquid diffusion coefficient. According to the results of spectrophotometric measurements, the dissolution of In does not lead to photochromic shifts in the ultraviolet or visible regions of the spectrum of the initial solution of AHC; this indicates that the associates formed are unstable. Thus, AHC acts by a film mechanism. The decrease in the efficiency of AHC upon an increase in the E value can be explained by two reasons. On the one hand, as E increases, the positive charge of the surface also increases (the zero charge potentials for In and Sn are −0.86 V and −0.64 V *vs* saturated silver chloride electrode, respectively); this hampers the initial electrostatic adsorption of the acridinium cation. On the other hand,

Table 1. Temperature dependence of the kinetic parameters of indium dissolution from the alloy and the potentials (E) for solutions not containing (—) or containing AHC

Parameter	$E = -0.58$ V								$E = -0.52$ V							
	25 °C		40 °C		45 °C		65 °C		25 °C		40 °C		45 °C		65 °C	
	—	AHC	—	AHC	—	AHC	—	AHC	—	AHC	—	AHC	—	AHC	—	AHC
$\tau_{t,2}$/s	80.0	900.0	—	420.0	—	120.0	—	25.0	—	—	—	—	—	—	—	—
i_t/A m^{-2}	140.0	39.0	—	56.0	—	75.0	—	147.0	—	—	—	—	—	—	—	—
τ_{se}/min	15.0	80.0	3.0	70.0	2.0	60.0	1.2	20.0	7.0	10.0	5.0	7.0	2.0	3.0	0.6	1.0
i_{se}/A m^{-2}	72.0	4.4	152.0	5.0	203.0	6.0	296.0	24.0	167.0	112.0	207.0	149.0	371.0	270.0	716.0	497
q_{se}/mC m^{-2}	98.0	102.0	80.0	110.0	60.0	126.0	31.0	98.0	93.0	104.0	88.0	92.0	60.0	65.0	34.0	35.0
τ_{min}/min	50.0	—	70.0	—	—	—	—	—	15.0	18.0	15.0	50.0	15.0	60.0	15.0	70.0
i_{min}/A m^{-2}	55.0	—	63.0	—	—	—	—	—	132.0	106.0	137.0	118.0	147.0	130.0	159.0	141.0
τ_{max}/h	2.6	—	2.2	—	—	—	—	—	1.5	1.0	1.5	1.2	1.3	1.7	1.2	1.7
i_{max}/A m^{-2}	58.0	—	65.0	—	—	—	—	—	154.0	115.0	183.0	125.0	197.0	135.0	218.0	145.0
τ_{max}/τ_{min}	3.2	—	1.8	—	—	—	—	—	6.0	3.2	6.0	1.4	5.3	1.6	4.6	1.4
i_{max}/i_{min}	1.1	—	1.1	—	—	—	—	—	1.2	1.1	1.3	1.1	1.3	1.0	1.4	1.0
$\Delta\tau_1 = \tau_{min} - \tau_{se}$ /min	35.0	—	67.0	—	—	—	—	—	8.0	5.0	10.0	40.0	13.0	56.0	14.0	69.0
$\Delta\tau_2 = \tau_{max} - \tau_{min}$ /min	110.0	—	60.0	—	—	—	—	—	75.0	45.0	75.0	36.0	65.0	40.0	55.0	30.0
$P \cdot 10^{-2}$/A m^{-2}	1.7	0.6	3.1	0.8	3.3	0.9	6.3	1.7	3.3	2.5	5.7	3.1	7.6	5.6	14.3	7.8
Q/A $\cdot$ (m^{-2} s$^{-1/2}$)	3.0	0.9	10.0	1.2	11.0	1.4	34.0	3.8	8.0	5.0	21.0	7.0	36.0	22.0	115.0	37.0
$D_{In} \cdot 10^{13}$/m^2 s^{-1}	6.3	1.7	7.0	2.0	7.5	2.5	10.7	4.0	14.0	12.9	18.2	15.3	19.6	15.5	24.1	20.6

Note. Dashes mean that the corresponding sections of the schematic current—time transient are missing (see Fig. 1). The transition time $\tau_{t,1}$ is observed only in the presence of AHC and at $E = -0.58$ V and amounts to 25 s irrespective of the temperature.

Table 2. Dependence of the activation energy (W/kJ mol^{-1}) on time (τ) and the potential (E) in solutions containing no AHC

τ	$E = -0.58$ V		$E = -0.52$ V			
/min	W_{3-4}	W_{4-5}	W_{3-4}	W_{4-5}	W_{5-6}	W_{6-7}
0.1	22.4		23.4			
0.5	21.7		20.7			
1.0	18.0		22.0	15.3		
2.0	14.6	11.3	16.6	11.5		
3.0	16.3	9.0	14.6	6.4		
5.0		9.6		6.0		
10.0		8.4		5.1		
20.0		8.2			6.4	
50.0		8.4			6.7	
80.0		8.4			7.5	
100.0		8.4				5.7
140.0		8.4				5.3
180.0		8.4				7.1

Note. Indices at the W value correspond to the numbers of sections of the current—time transient (see Fig. 1).

Table 3. Dependence of W_D and D_0 on E and on the presence of AHC

E/V	Solution	W_D/kJ mol^{-1}	$D_{In}{}^0$/m^2 s^{-1}
−0.58	0	11.5	$6.4 \cdot 10^{-11}$
−0.58	AHC	22.9	$1.3 \cdot 10^{-9}$
−0.52	0	11.5	$1.5 \cdot 10^{-9}$
−0.52	AHC	9.9	$6.2 \cdot 10^{-11}$

according to voltammetry, $E = -0.58$ V corresponds to the transition of the alloy to salt passivation, while $E = -0.52$ V lies in the region of stable salt passivation. Apparently, the film formed by the inhibitor cannot compete substantially with a salt film. Hence, the introduction of AHC into the solution virtually does not change the current—time transient pattern at $E = -0.52$ V, whereas at $E = -0.58$ V, it results in the disappearance of section *4—7* at 25—40 °C and in the appearance of sections *1—2* and *2—3* at any T value.

The kinetic equation for section *1—2* has the following form:[2]

$$i_{In} = 3F[In]_0 \sqrt{D_{In^{3+}}/\pi\tau}\, \exp(2{,}3\Delta E_0/b_a) = \\ = \beta\tau^{-1/2} \sqrt{D_{In^{3+}}}\,. \tag{7}$$

Under the conditions considered, the i—$\tau^{-1/2}$ straight lines can be described by relation (8), which points to a dependence of $D_{In^{3+}}$ on τ.

$$i_{In} = i_{In,0} + \rho_i\tau^{-1/2} \tag{8}$$

From relations (7) and (8), it follows that

$$\sqrt{D_{In^{3+}}} = (\rho_i + i_{In,0}\tau^{1/2})/\beta = \sqrt{D_{In^{3+},0}} + \rho_D\tau^{1/2}. \tag{9}$$

Table 4. Dependence of $D_{In^{3+}}$ and δ on T and τ and the dependence of the constants of Eqs. (8) and (9) on T

Section	Parameter	25 °C	40 °C	45 °C	65 °C
1—2	$D_{In^{3+}} \cdot 10^{12}$/m^2 s^{-1} ($\tau = 2$ s)	1.3	2.3	4.1	23
1—2	$D_{In^{3+}} \cdot 10^{11}$/m^2 s^{-1} ($\tau = 25$ s)	0.6	1.5	2.7	10
1—2	$i_{In,0}$/A m^{-2}	27	47	67	115
1—2	ρ_i/A s$^{-1/2}$ m^{-2}	51	45	57	190
1—2	$\sqrt{D_{In^{3+},0}} \cdot 10^7$ /m s$^{-1/2}$	8.0	8.8	10	26
1—2	$\rho_D \cdot 10^7$/m s^{-1}	4.4	9.3	10.6	15
2—3	$D_{In^{3+}}/\delta \cdot 10^7$/m s^{-1}	2.9	4.2	5.7	11
2—3	$\delta \cdot 10^5$/m	1.9	3.6	4.7	9.1
3—4	$D_{In^{3+}}/\delta \cdot 10^7$/m s^{-1}	4.8	5.9	6.8	13

In this system of coordinates, $\sqrt{D_{In^{3+}}}$ — $(\rho_i + i_{In,0}\tau^{1/2})$, for each particular $[In]_0$, irrespective of the E and T values, we obtain one straight line starting from the origin of coordinates with a slope of $1/\beta$. The constants of the equations obtained are related to one another as

$$i_{In,0} \sqrt{D_{In^{3+},0}} = \rho_i\rho_D. \tag{10}$$

Since $\rho_i > 0$ and $\beta > 0$, it should be expected that $D_{In^{3+}}$ would increase with τ. This is consistent with the results of calculations (Table 4), which also confirm the validity of relation (10).

The calculated $D_{In^{3+}}$ values are substantially lower than the diffusion coefficients for ions in water ($7 \cdot 10^{-10}$ m^2 s^{-1}). They can be interpreted as effective values for the diffusion of ions through a film formed mostly at $\tau < \tau_{t,1}$. The increase in $D_{In^{3+}}$ with τ can be explained by the fact that the film becomes loose as its thickness increases with time.

Kinetic Eq. (11)[2] makes it possible to estimate the film thickness δ in section *2—3*; it is assumed that the $D_{In^{3+}}$ value does not change on going from section *1—2* to section *2—3* (see Table 4).

$$i_{In} = \beta \sqrt{\pi}\, D_{In^{3+}}/\delta \tag{11}$$

For the range of mixed kinetics *3—4*, the $D_{In^{3+}}/\delta$ values were calculated from Eq. (2) taking into account the fact that, according to the powder X-ray diffraction data, it can be approximately considered that $[In]_S \approx 0.2[In]_0$.[6]

Thus, AHC forms a protective film on the surface and thus decreases i_{In} and, correspondingly, the concentration of irreversible vacancies; hence, it retards the solid-state diffusion and inhibits the selective dissolution of alloys. Simultaneously, it changes the τ_{se} and i_{se} values. Let us consider the possible reasons for the influence of AHC on the phase rearrangement and, as a

Table 5. Dependence of K_X on T

T/°C	$E = -0.58$ V				$E = -0.52$ V			
	$K_{D_{\mathrm{In}}}$	$K_{\tau_{\mathrm{se}}}$	$K_{q_{\mathrm{se}}}$	$K_{\mathrm{In}_{\mathrm{min}}}$	$K_{D_{\mathrm{In}}}$	$K_{\tau_{\mathrm{se}}}$	$K_{q_{\mathrm{se}}}$	$K_{\mathrm{In}_{\mathrm{min}}}$
25	3.7	0.2	1.0	—	1.1	0.7	0.9	1.2
40	3.5	0.4	0.7	—	1.2	0.7	0.8	1.2
45	3.0	0.4	0.5	—	1.3	0.7	0.9	1.1
65	2.7	0.6	0.4	—	1.2	0.5	1.0	1.1

consequence, on the surface enhancement. In the general case, these processes are determined by the kinetic factor, *i.e.*, by the rate of the fluctuational formation of the new phase, and by the thermodynamic factor, namely, by the activity of the more positive component of the alloy in the irreversible surface layer, which depends on the concentration of vacancies.[7,8] Acridine hydrochloride can exert a dual influence on the phase rearrangement. This compound can retard the process by decreasing the concentration of irreversible vacancies, which is manifested in the decrease in D_{In} (see Table 1); however, this additive can also accelerate the phase rearrangement acting as a surfactant. This is caused by a decrease in the interfacial tension energy (σ) and, correspondingly, an increase in the rate of formation of N two-dimensional nuclei of the new phase with a higher content of the positive component, according to Eq. (8):

$$N = N_0\exp(k_N\sigma^2/\Delta\mu), \qquad (12)$$

where N_0 and k_N are constants and $\Delta\mu$ is the supersaturation of crystallization. To estimate the effect of AHC on the characteristics of dissolution of the alloy, let us introduce the parameter $K_X = X/X_{\mathrm{AHC}}$, where X and X_{AHC} are the solid-state diffusion coefficient D_{In} and the time of surface enhancement τ_{se} in solutions without and with AHC, respectively (Table 5).

It follows from Table 5 that AHC retards both the phase rearrangement and surface enhancement. This implies that the factors of the concentration of irreversible vacancies and the activity of the more positive component in the near-surface layer predominate. They are more significant at $E = -0.58$ V and become less significant as T increases. The $K_{i,\mathrm{In}}$ values at $E = -0.52$ V are consistent with the foregoing; they lie in the range between 1.1 and 1.5 and virtually do not depend on τ. At $E = -0.58$ V, they are markedly greater and increase as the protective film is formed from 2.5—4.0 at $\tau < 30$ min to 200—400 at $\tau > 2.5$ h.

Thus, when the temperature is raised, the phase rearrangement in the alloy and the surface enhancement are accelerated, which requires a smaller critical charge and points to easier accumulation of structural defects.

The increase in the time needed to attain the current minimum in the current—time transient upon an increase in the temperature and the corresponding increase in the time needed to reach the subsequent current maximum indicate that the increase in the diffusion rate predominates over the surface enhancement.

The protective action of AHC decreases with an increase in the potential. At $E = -0.58$ V, AHC forms an activation barrier to the diffusion, whose effect predominates over the decrease in the entropy constituent of D_{In}. In the salt passivation region ($E = -0.52$ V), AHC virtually does not compete with the salt film and enhances it very slightly. The influence of AHC is determined by the entropy constituent of D_{In}.

References

1. V. V. Losev, A. P. Pchel'nikov, and A. I. Marshakov, in *Itogi Nauki i Tekhniki. Elektrokhimiya* [*Advances in Science and Engineering. Electrochemistry*], VINITI, Moscow, 1984, **21**, 77 (in Russian).
2. I. K. Marshakov, A. V. Vvedenskii, V. Yu. Kondrashin, and G. A. Bokov, *Anodnoe rastvorenie i selektivnaya korroziya splavov* [*Anodic Dissolution and Selective Corrosion of Alloys*], Izd-vo Voronezh Gos. Univ., Voronezh, 1988, 204 pp. (in Russian).
3. A. V. Vvedenskii, Sc. D. (Chem.) Thesis, Voronezh Gos. Univ., Voronezh, 1994, 354 pp. (in Russian).
4. A. G. Berezhnaya and V. V. Ekilik, *Elektrokhimiya*, 1991, **27**, 655 [*Sov. Electrochem.*, 1991, **27** (Engl. Transl.)].
5. A. P. Pchel'nikov, A. I. Marshakov, and V. V. Losev, *Elektrokhimiya*, 1985, **21**, 949 [*Sov. Electrochem.*, 1985, **21** (Engl. Transl.)].
6. V. V. Ekilik, M. G. Komakhidze, A. G. Berezhnaya, and N. G. Sudorgin, *Zashchita Metallov*, 1997, **33**, 384 [*Protect. Met.*, 1997, **33** (Engl. Transl.)].
7. I. D. Zartsyn, A. V. Vvedenskii, I. K. Marshakov, and N. V. Storozhenko, *Zashchita Metallov*, 1991, **27**, 3 [*Protect. Met.*, 1991, **27** (Engl. Transl.)].
8. M. Fol'mer, *Kinetika obrazovaniya novoi fazy* [*Kinetics of the Formation of a New Phase*], Nauka, Moscow, 1986, 315 (in Russian).

Received December 5, 1997